



First principles study on the structure and STM image of acetylene adsorption on Ge(0 0 1)

X.L. Fan^{a,*}, Q.Z. Cheng^a, S. Ahmad^a, Y.F. Zhang^b, W.M. Lau^{c,d}

^a School of Material Science and Engineering, Northwestern Polytechnical University, 127 YouYi Road West, Xian, 710072 Shaanxi, China

^b Department of Chemistry, Fuzhou University, Fuzhou 35002, China

^c Surface Science Western, University of Western Ontario, London, Ontario, Canada N6A 5B7

^d Beijing Computational Science Research Center, Beijing 100084, China

ARTICLE INFO

Article history:

Received 2 July 2011

In final form 14 August 2011

Available online 19 August 2011

ABSTRACT

The adsorption of acetylene on Ge(0 0 1) is investigated by first-principles calculations. The calculations of total energy and simulations of scanning tunneling microscopic images consistently show that the two binding features observed experimentally are di- σ and paired-end-bridge configurations, instead of p-bridge structure. In addition, the bias-dependent STM images and the electronic states from the adsorbed molecule and bare Ge atoms above the surface have been calculated to clarify what cause the adsorbed molecule appear darker than the bare Ge atoms. Particularly, we caution that all features in STM imaging have been adequately simulated by the Tersoff–Hamann theory except tip–sample interactions.

© 2011 Elsevier B.V. All rights reserved.

1. Introduction

In the last decades, great efforts have been devoted to study the interaction of unsaturated hydrocarbon molecules on semiconductor wafer surfaces [1], such as acetylene and ethylene with Si(0 0 1). In comparison, the interaction of hydrocarbons with Ge(0 0 1) was far less studied. In reference to Si(0 0 1), Ge(0 0 1) has the same lattice structure except having a slightly larger lattice constant. Further, the electronic structures of the two surfaces were also believed to be very similar. However, according to recent studies [2–4], these two surfaces exhibit quite different physical and chemical behaviors, with examples including the detailed reaction pathways, adsorption configurations, and scanning tunneling microscopic (STM) images [2–5]. Since the electron mobility in Ge is higher than that in Si, it is conceivable that faster devices can be produced by replacing Si with Ge. Because of this, the current quest of organic–inorganic hybrid microelectronics/optoelectronics has driven the study of bare Ge surface [6–8], also the comparative study of unsaturated hydrocarbon molecules on Ge and Si [9–11].

In the subject of hydrocarbon adsorption on Ge(0 0 1), the adsorption of ethylene (C_2H_4) is the best known case. The previous STM and temperature program desorption (TPD) investigation by Kim et al. [12], as well our first-principles calculations [13] consistently show that the di- σ and paired-end-bridge configurations are the two distinct bonding geometries for C_2H_4 on Ge(0 0 1). The

adsorption of acetylene (C_2H_2) on Ge(0 0 1) is considerably more intriguing than that of C_2H_4 because in addition to the interdimer di- σ and intradimer end-bridge configurations, the following two additional adsorption models are believed to be probable [14]: the p-bridge and r-bridge configurations. These $C_2H_2/Ge(0 0 1)$ configurations are depicted in Figure S1 (see Supporting information). In both the r-bridge and p-bridge configurations, the two C atoms of C_2H_2 molecule are bonded to the four Ge atoms of the two adjacent surface dimers by forming four σ bonds, thus they are also named tetra- σ configurations. The distinction between the two tetra- σ configurations is the alignment orientation of the C–C axis, which is parallel to the Ge–Ge dimer bond in the p-bridge configuration and perpendicular to the C–C dimer bond in the r-bridge configuration. When Kim et al. [14] observed two adsorption configurations for C_2H_2 on Ge(0 0 1) using the STM and TPD, they labeled them as ‘Feature A’ and ‘Feature B’. Feature A was assigned to the di- σ configuration, and Feature B to the p-bridge configuration. However, the interpretation of the configuration of Feature B was challenged by the theoretical calculations of Cho and Kleinman [15], as they assigned Feature B to a paired-end-bridge structure. More interestingly, when they changed the filled state imaging from -1.8 V to -1.4 V, the tunneling current signals from the Ge dimer associated with C_2H_2 molecule for Feature A decreased drastically such that the corresponding STM protrusions changed to STM depressions [14]. This intriguing change induced by the reduction of STM bias was also observed for Feature B in very low bias. This bias-dependence and the contrast inversion in STM images have never been examined theoretically.

This work aims to clarify: (a) the C_2H_2 adsorption configurations on Ge(0 0 1); (b) the interpretation of the experimental STM

* Corresponding author. Fax: +86 029 88490502.

E-mail address: xlfan@nwpu.edu.cn (X.L. Fan).

images of $C_2H_2/Ge(001)$, and especial the root causes for the darker images. To accomplish these goals, we apply the first-principles method based on the density functional theory (DFT) to study the configuration for each possible adsorption together with the total-energy analysis and STM image simulation. Furthermore, we also exploit the meticulously measured STM images at different bias by Kim et al. [14], with our calculations of partial charge density, to clarify the underlying surface physics and chemistry on the adsorption of C_2H_2 on $Ge(001)$.

2. Calculation methods

The geometry optimization and electronic structure calculations in the present study were performed on the basis of density functional theory with applying the Vienna ab initio simulation package (VASP) [16–19]. The setup was similar with our previous study for $C_2H_4/Ge(001)$ [13], the reported calculations have been carried out using the Vanderbilt ultrasoft pseudopotential [20–22] and plane-wave method with cutoff energy of 350 eV. The generalized gradient approximation (GGA) [23] of Perdew–Wang (PW91) has been used for the electronic exchange–correlation potential. The STM images was calculated using Tersoff–Hamann theory [24].

The $Ge(001)$ surface has been modeled by a slab, with a unit cell of $8.1 \times 8.1 \times 23.0 \text{ \AA}$, containing eight Ge atomic layers and a vacuum region of 12.94 \AA spacing. The top of the slab is a $p(2 \times 2)$ unit with two asymmetric Ge dimers. The structure optimization were performed using the calculated bulk lattice constant of 5.75 \AA , and the Ge atoms in the bottom layer of the slab, as well as the terminating hydrogen atoms were fixed to the bulk position. In the total energy calculations, the Brillouin zone was sampled by a Monkhorst–Pack scheme with $4 \times 4 \times 1$ k-point grids, and the convergence criteria of 1×10^{-5} eV for the SCF energy and 0.04 eV/\AA for force have been used throughout.

3. Results and discussions

3.1. Adsorption configurations of C_2H_2 on $Ge(001)$ surface

We have calculated both the two configurations of the interdimer on-top di- σ configuration and intradimer end-bridge configuration at 0.5 ML and 1.0 ML coverage. The corresponding adsorption energies are listed in Table 1. The respective adsorption energies of the di- σ and end-bridge configurations are 1.59 and 1.52 eV at 0.5 ML; hence, they are very similar, with the di-configuration being more stable by 0.07 eV. When the coverage increases to 1.0 ML, the paired-di- σ configuration and paired-end-bridge configuration are formed. Our calculations show that the paired-end-bridge configuration is more stable than the paired-di- σ configuration by 0.32 eV at 1.0 ML. Our calculated adsorption energies for the two binding geometries at 0.5 and 1.0 ML coverage are consistent with the previous first-principles calculations as listed in Table 1.

In addition to the above adsorption configurations, the two tetra- σ configurations, i.e., the r-bridge and p-bridge structures have also been studied. The adsorption energy of the r-bridge structure

is only 0.07 eV, and the adsorption of the p-bridge structure is endothermic with the adsorption energy of -0.23 eV. Hence, it is unlikely for the p-bridge structure to present on $Ge(001)$. In fact, our calculations show that when the optimized structure of the p-bridge structure is formed, the repulsive interactions between the parallel C–C bond and two Ge–Ge bonds lead to the elongation of both the C–Ge and C–C bonds relative to those of the more stable r-bridge structure. In short, the interpretation of Kim et al. [14], of $C_2H_2/Ge(001)$ must be revised.

In summary, the most stable adsorption configurations should be the interdimer on-top di- σ configuration and intradimer end-bridge configuration at 0.5 ML, both with adsorption energy larger than 1.5 eV. When the coverage increases to 1.0 ML, the paired end-bridge configuration should be the most stable one but di- σ and paired-di- σ can co-exist. The p-bridge structure is endothermic and unstable and the r-bridge structure has small adsorption energy of 0.19 eV.

3.2. Simulated scanning tunneling microscopy images

According to our total energy calculations, the presence of p-bridge configuration is unlikely for $C_2H_2/Ge(001)$. Thus, Feature B observed in the STM experiments of Kim et al. cannot be described as the p-bridge configuration. In order to find out which one of the adsorption configurations gives the observed Feature B, we have simulated the filled state STM images for seven possible adsorption configurations with bias voltage at -1.5 V.

Firstly, as a benchmark reference for the $C_2H_2/Ge(001)$, the STM image of the bare $Ge(001)p(2 \times 2)$ surface has been computed with bias voltage at -1.5 V; the results are summarized in Figure 1a. The bright protrusions in Figure 1a denote the high charge densities centered on the up-Ge atom of the dimer, which are derived from the occupied dangling bond of the up-Ge atom formed from its pz orbital. Our simulated images are consistent with the experimental STM observations and theoretical simulations of the STM images for the $Ge(001)$ surface [8].

Figure 1b and c show the respective simulated images of filled states at bias of -1.5 V for the di- σ and end-bridge configuration at 0.5 ML. Both images show the bright protrusions centered on the C_2H_2 molecule and up-Ge atom of the unreacted dimer (no C_2H_2 adsorption). However, the pattern of the protrusions on top of the C_2H_2 molecule are different in the two images. For the di- σ configuration, the pattern is parallel to the dimer axis, but for the end-bridge configuration, the pattern is perpendicular to the dimer axis. Our simulated images for the paired-di- σ and paired-end-bridge configurations are shown in Figure 1d and e. The image of the paired-di-structure shows the protrusions with parallel bright bean-shaped spot on top of the two adjacent dimers reflecting the pattern of each C_2H_2 molecule adsorption on every dimer site. For the paired-end-bridge configuration, the image shows protrusion along the direction of the dimer axis located between two adjacent dimers in the same dimer row, which corresponds to the two adsorbed molecules bridging the two adjacent dimers. In addition, we note that simulations at bias voltage higher than -1.5 V have been performed but do not give any more insightful information. Because DFT calculations typically underestimate the band-gap energy of semiconductor, the best image match of simulated results to experimental results are generally found with the tip bias for the simulations smaller than the experimental condition. For example, in the high bias group, our simulated results at -1.5 V best match the experimental results at -1.8 V. Similarly in the low bias group, our simulated results at -1.0 V best match the experimental results at -1.4 V.

The simulated images for the two tetra- σ configurations at -1.5 V are shown in Figure 1f. The image of r-bridge configuration shows two round protrusions on top of the two C atoms between

Table 1

Calculated adsorption energies (in eV) per C_2H_2 molecule on $Ge(001)$. Previous calculation results are listed for comparison.

	Di- σ		End-bridge		r-Bridge	p-Bridge
	0.5 ML	1.0 ML	0.5 ML	1.0 ML		
This GGA	1.59	1.57	1.52	1.89	0.19	-0.23
Cho and Kleinman ^a	1.78	1.81	1.64	1.87	0.24	-0.03

^a Ref. [15].

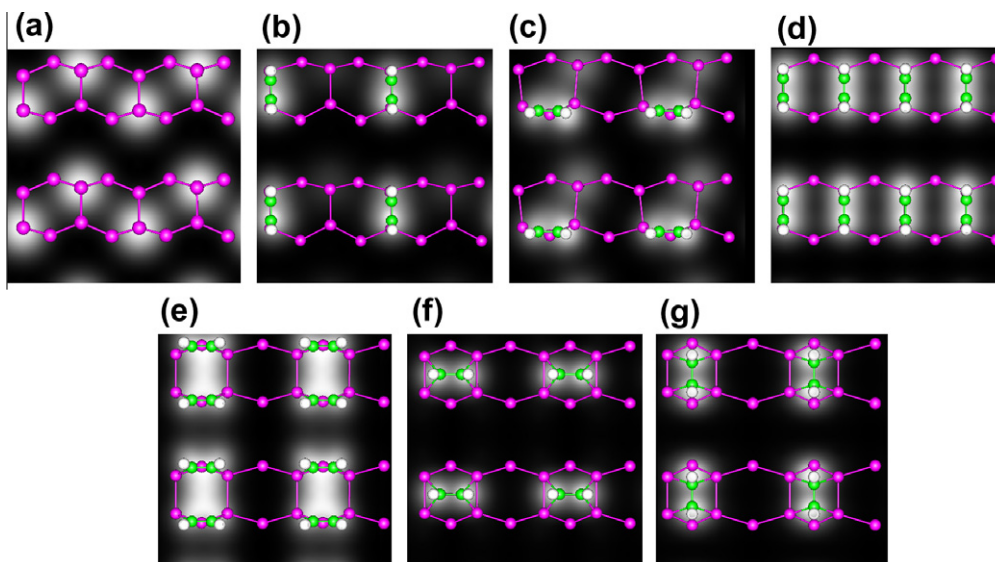


Figure 1. The simulated filled-state STM images at bias of -1.5 V for: (a) clean $\text{Ge}(001)p(2 \times 2)$ surface; (b) di- σ $\text{C}_2\text{H}_2/\text{Ge}(001)$ at 0.5 ML; (c) end-bridge $\text{C}_2\text{H}_2/\text{Ge}(001)$ at 0.5 ML; (d) paired-di- σ $\text{C}_2\text{H}_2/\text{Ge}(001)$; (e) paired-end-bridge $\text{C}_2\text{H}_2/\text{Ge}(001)$; (f) r-bridge $\text{C}_2\text{H}_2/\text{Ge}(001)$; and (g) p-bridge $\text{C}_2\text{H}_2/\text{Ge}(001)$.

two adjacent dimers. As shown in Figure 1g, the pattern of the p-bridge structure is similar with the pattern of the r-bridge structure, except that the alignment of the axis connecting the two protrusions are different, which is perpendicular and parallel to the axis of the Ge–Ge dimer in the r-bridge and p-bridge structure, respectively. Both are consistent with the alignment of the C_2H_2 molecule.

Among the above simulated images shown in Figure 1b–g, the image of the di- σ structure in Figure 1b has the same pattern as Feature A observed in the STM experiment reported by Kim et al. [14]. The simulation results also confirm that Feature B really cannot be assigned to the p-bridge configuration and this assignment by Kim et al., has to be revised. For Feature B, Kim et al. showed that the plots of the constant current tip height shows two deep minimum with a rise in height between them along the center of the dimer row and perpendicular to the dimer row. However, our simulated image for the p-bridge configuration in Figure 1g shows two protrusions on top of the two C atoms of the dimer with a ‘valley’ between them in the direction perpendicular to the dimer row and between two adjacent dimers. Our STM simulations of the p-bridge geometry is consistent with the charge density result calculated by Cho and Kleinman [15], the plot of charge density shows a minimum along the center of the dimer row. This is exactly opposite to the reported characteristics of Feature B. With a thorough analysis of all simulated images, we find that our simulated images of the paired-end-bridge structure in Figure 1e closely match the characteristics of Feature B.

3.3. Attempts to interpret the STM images at low bias

Although the electronic structure is the major factor in the STM imaging, however, the bias dependence of the image, as well as the effect of the atomic structure on the imaging cannot be studied through the charge density calculated by Cho and Kleinman [15]. According to the observations in the STM experiment, both Feature A and Feature B appear as protrusion at bias of -1.8 V; but at the low bias voltage of -1.4 V, the bright protrusions in the two images change to depressions or dark spots. In view of this, we have further calculated the STM images for the di- σ and paired-end-bridge configurations at low bias in this section, and try to analyze the root cause of depressions or darker.

The STM image of the di- σ structure at bias of -1.0 V is shown in Figure 2a. Although the contrast between the C_2H_2 molecule and the bare Ge atom is reduced relative to the STM image at bias of -1.5 V in Figure 1b, still the C_2H_2 molecules are imaged as protrusion. In fact, none of our simulated images for the di- σ structure show the experimental observed depressions. As for the paired-end-bridge structure, in order to display the relative height of the adsorbed molecule and bare Ge atom in the STM image, the paired-end-bridge configuration has been recalculated using a double size supercell with two bare Ge–Ge dimers. The respective STM images at biases of -1.5 and -1.0 V are shown in Figure 2b and c. Figure 2b shows both the C_2H_2 molecules and bare up-Ge atoms are imaged as protrusions with similar brightness at bias of -1.5 V. When the bias decreases to -1.0 V, as shown in Figure 2c, the images are darker and lower above the molecules than above the bare Ge atoms, which is qualitative consistent with the experimental observations. Actually, the STM experiments reported in the literature on $\text{C}_2\text{H}_2/\text{Ge}(001)$ were done at room temperature. With such condition, the unreacted surface dimer is known to be symmetric. In comparison, theoretical studies typically adopt the most stable reconstructed structure ($p(2 \times 2)$ or $c(4 \times 2)$) to model the $\text{Ge}(001)$ surface, a structure in which the Ge–Ge dimers are buckled, as shown in our simulated STM images. The calculated images in Figure 2a and b look exactly the same as the Feature A and Feature B if the bare buckled dimer is replaced as the symmetric dimer.

In order to analyze why our simulated results based on the DFT derived Tersoff–Hamann theory cannot find the STM images of ‘depressions’ for the di- σ structure at low biases, we have further calculated the line profile of the partial charge density of the C_2H_2 molecule and bare Ge atom because these results give the respective contributions of the electronics states of the molecule and bare Ge dimer above the surface within the concerned energy region. Again we highlight that in the STM experiment, the di-structure appears as protrusions at bias of -1.8 V, and change to depressions at -1.4 V. Accordingly, we have calculated the line profile of the electronic states included in three biases of -2.0 , -1.5 and -1.0 V for both the di- σ and paired-end-bridge configurations, as shown in Figures 3 and S2. The three line profiles in each figure represent the values of the partial charge density along the vertical lines through the C and H atoms of the C_2H_2 molecule and bare Ge

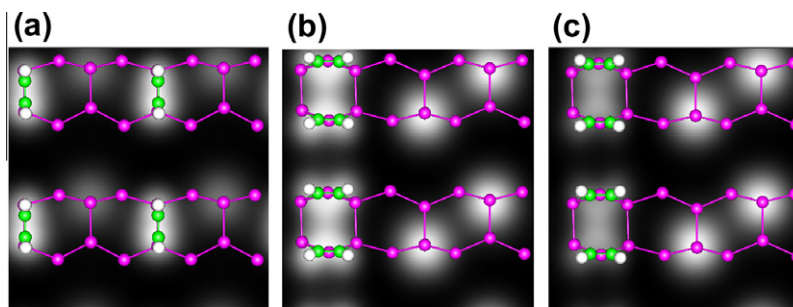


Figure 2. The simulated filled-state STM images for $C_2H_2/Ge(001)$; (a) di- σ at 0.5 ML at bias of -1.0 V; (b) paired-end-bridge at bias of -1.5 V; and (c) paired-end-bridge at bias of -1.0 V.

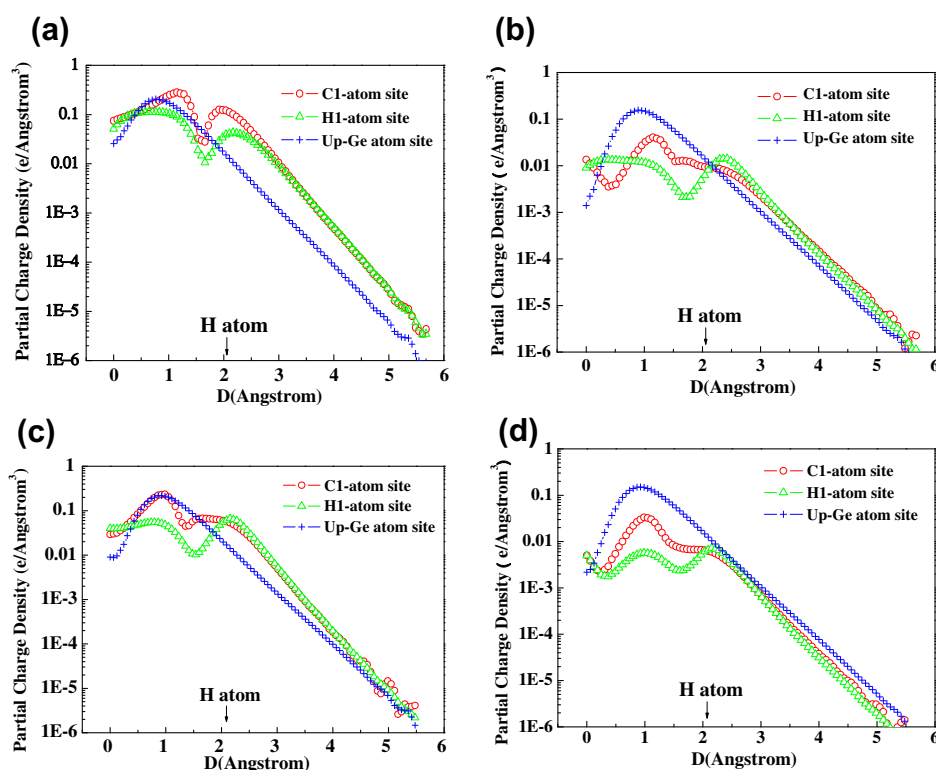


Figure 3. Vertical line profiles of calculated partial charge density versus distance from the $Ge(001)$ surface for the di-structure at bias of (a) -2.0 V; (b) -1.0 V; and paired-end-bridge structure at bias of (c) -2.0 V; (d) -1.0 V. Three curves in each figure representing the partial charge density on the vertical lines through H, C and up-Ge atom sites are shown. The arrow indicates the height of the top H atom of the C_2H_2 molecule adsorbed on $Ge(001)$.

atoms. For the di- σ structure at high bias of -2.0 V as shown in Figure 3a, the line value of charge density through the C atom is the largest. When the bias reduces to -1.5 V in Figure S2a, the largest values of the charge density of the C_2H_2 molecule and bare Ge atom are almost the same. At low bias of -1.0 V, Figure 3b shows that the line value of charge density through the bare up-Ge atom is the largest, and the charge density of the molecule reduces a lot relative to the value at high bias. These line profiles show that although the major electronic states of the molecule are located below -1.5 V, there are still some states locating between -1.5 V and -1.0 V. However, as shown in the simulated image in Figure 2a, the charge and current above the molecule are still higher than those of the bare Ge atom even at the low bias of -1.0 V. This topographic effect is not surprising because the charge density of the molecule expand further into the vacuum region above the surface, as displayed in Figure 3b where the charge density associated with the C and H atoms of the C_2H_2 molecule is larger than those of the bare Ge atom above the top H atom. The similar situation has also

been reported for the alkane-thiol molecule on the $Au(111)$ surface [25], where although the major electronic states near the EF comes from the thiol atom, the STM images show the tail CH_3 group because the tail group are closer to the STM tip.

For the paired-end-bridge configuration, the line profile of the charge density at bias voltages of -2.0 , -1.0 and -1.5 V are shown in Figures 3c and S2b, respectively. The charge density of the C_2H_2 molecule is only slightly larger than that of the bare Ge atom at -2.0 V. When the bias decreases to -1.5 V, as shown in Figure S2b, the charge of the C_2H_2 molecule reduces a lot and the charge of the bare up-Ge atom only reduces a little. When the tip is above the top H atom, the charge and current above the molecule and the bare Ge atom are almost the same. At -1.0 V, Figure 3d shows that the charge density of the C_2H_2 molecule further reduces. Unlike the situation of the di- σ structure, the charge and current above the molecule have already become smaller than those of the bare Ge atoms, which is indeed displayed in the simulated STM image in Figure 2c as the molecules appear darker than the bare up-Ge atoms.

Our calculated line profiles demonstrate that both the electronic structure and topographic factor of elements on the surface are properly displayed in the simulated STM images generated by the Tersoff–Hamann Theory. But with this method, we cannot find the depressions appearing above the di- σ structures in the STM experiment with bias changing from -1.8 V to -1.4 V. Actually, there are cases for which the STM images cannot always be described within the Tersoff–Hamann approximation. When the tip is close enough to the surface to form a kind of bonding with it, such a strong tip–sample interaction can lead to contrast inversion in STM images on metallic surfaces [26]. Even when the tip is not so close to sample that the tip–sample bonding is small, the tip-induced electronic field may change the electronic structure of the sample surface. Interestingly, similar ‘depression’-like features above the adsorbed molecule have also been observed [27] previously in the case of $C_2H_4/Si(001)$, and the electronic structures of $C_2H_4/Si(001)$ have been calculated by Ness and Fisher [28] to explain such features. It turns out that a tip-induced electric field makes the charge and current above the adsorbed molecules smaller than the bare Si dimers; consequently, the STM image of the molecule can appear as depressions.

In the present case, the di- σ adsorbed molecule is closer to tip than the end-bridge adsorbed molecule by about 0.2 Å according to our calculation, thus the influence of the electron field induced by the tip will be much stronger on the di- σ structure than on the paired-end-bridge structure. Further considering with the similarity between the $Si(001)$ and $Ge(001)$ surface, tip–surface interactions may be one possible cause for depression above the di- σ structure at low bias voltage observed by Kim et al. [14] which beyond the Tersoff–Hamann approximation.

4. Conclusions

Both our calculated adsorption energies and STM images consistently show that the di- σ and paired-end-bridge structures are the two stable adsorption geometries discovered in the STM experiments. The investigation of the bias-dependent images and line profile of the charge density of the adsorbed C_2H_2 molecule and bare Ge atom show us the STM image are not only the combined results of the atomic and electronic structure of both the surface and adsorbed molecule, but also influenced by the tip–sample interaction. At low bias, the contribution of electronic states from the adsorbed molecules is less than the contribution from the bare Ge atoms in both the two structures, which leads the adsorbed molecule appearing darker in the paired-end-bridge structure. However, the charge and current above the di- σ adsorbed

molecule is still larger than those above the bare Ge atoms, in this case, tip–sample interaction is the major cause for the depressions.

Acknowledgments

This work was funded by the Discovery Grant program of the Natural Science and Engineering Research Council of Canada (NSERC) for W.M. Lau, the National Natural Science Foundation of China (NSFC) (20903075) and funds from Shannxi Province (SJ08B14) for Xiaoli Fan. This work was also supported by the 111 Project (B08040) in China. The authors also acknowledge the support from Surface Science Western and the Faculty of Science at the University of Western Ontario.

Appendix A. Supplementary data

Supplementary data associated with this article can be found, in the online version, at [doi:10.1016/j.cplett.2011.08.034](https://doi.org/10.1016/j.cplett.2011.08.034).

References

- [1] R.A. Wolkow, *Annu. Rev. Phys. Chem.* 50 (1999) 413.
- [2] P.W. Loscutoff, S.F. Bent, *Annu. Rev. Phys. Chem.* 57 (2006) 467.
- [3] Y.E. Cho, J.F. Maeng, S. Kim, S. Hong, *J. Am. Chem. Soc.* 125 (2003) 7514.
- [4] M.A. Filler, C. Mui, C.B. Musgrave, S.F. Bent, *J. Am. Chem. Soc.* 125 (2003) 4928.
- [5] X.L. Fan, W.M. Lau, Z.F. Liu, *J. Phys. Chem. C* 113 (2009) 8786.
- [6] U. Schwingenschlogl, C. Schuster, *Chem. Phys. Lett.* 449 (2007) 126.
- [7] A. Houselt, R. Gastel, B. Poelsema, H. Zandvliet, *Phys. Rev. Lett.* 97 (2006) 266104.
- [8] M.W. Radny, G.A. Schofield, P.V. Smith, N.J. Curson, *Phys. Rev. Lett.* 100 (2008) 246807.
- [9] D.H. Kim, D.S. Choi, S. Hong, S. Kim, *J. Phys. Chem. C* 112 (2008) 7412.
- [10] Y.J. Hwang, E. Hwang, D.H. Kim, A. Kim, S. Hong, S. Kim, *J. Phys. Chem. C* 113 (2009) 1426.
- [11] J.H. Cho, E. Morikawa, *J. Chem. Phys.* 124 (2006) 024716.
- [12] A. Kim, D.S. Choi, J.Y. Lee, S. Kim, *J. Phys. Chem. B* 108 (2004) 3256.
- [13] X.L. Fan, C.C. Sun, Y.F. Zhang, W.M. Lau, *J. Phys. Chem. C* 114 (2010) 2200.
- [14] A. Kim, J.Y. Maeng, J.Y. Lee, S. Kim, *J. Chem. Phys.* 117 (2002) 10215.
- [15] J.Y. Cho, L. Kleinman, *J. Chem. Phys.* 119 (2003) 2820.
- [16] G. Kresse, J. Hafner, *Phys. Rev. B* 47 (1993) R558.
- [17] G. Kresse, J. Hafner, *Phys. Rev. B* 49 (1994) 14251.
- [18] G. Kresse, J. Furthmüller, *Phys. Rev. B* 54 (1996) 11169.
- [19] G. Kresse, J. Furthmüller, *Comput. Mater. Sci.* 6 (1996) 15.
- [20] D. Vanderbilt, *Phys. Rev. B* 41 (1990) 7892.
- [21] M.L. Cohen, *Phys. Rep.* 110 (1984) 293.
- [22] M.C. Payne, M.P. Teter, D.C. Allan, T.A. Arias, J.D. Joannopoulos, *Rev. Mod. Phys.* 64 (1992) 1045.
- [23] J.P. Perdew, in: P. Ziesche, H. Eschrig (Eds.), *Electronic Structure of Solids '91*, Akademie-Verlag, Berlin, 1991, p. 11.
- [24] T. Tersoff, D.R. Hamann, *Phys. Rev. B* 31 (1985) 805.
- [25] C.G. Zheng et al., *J. Chem. Phys.* 117 (2002) 851.
- [26] G. Doyen, D. Drakova, M. Scheffler, *Phys. Rev. B* 47 (1993) 9778.
- [27] A.J. Mayne, A.R. Avery, J. Knall, T.S. Jones, G.A.D. Briggs, W.H. Weinberg, *Surf. Sci.* 284 (1993) 247.
- [28] F. Ness, A.J. Fisher, *Phys. Rev. B* 55 (1997) 10081.